Mathematical applications associated with the deliberate release of infectious agents

Gerardo Chowell, Ariel Cintrón-Arias, Sara Del Valle, Fabio Sánchez, Baojun Song, James M. Hyman, Herbert W. Hethcote, and Carlos Castillo-Chávez

Abstract. Efforts to anticipate, prevent, or control deliberate releases of biological agents are critical components of homeland security research. The lack of data on deliberately induced epidemics naturally leads to the use of mathematical models (capable of simulating realistic scenarios) in the evaluation of policies that ensure our security. Modeling single outbreaks of a disease can help give insight into the effectiveness of our ability to respond and control such epidemics. We quantify the impact of delaying the response to an epidemic in a probabilistic network model and in compartmental differential equation models. Simulation studies are used to generate new insights on the dynamics of deliberate releases. In these settings we can explore ways of diminishing the impact of unexpected releases after detection. We review mathematical models that account for public health interventions and individual behavioral changes or incorporate the impact of "transient" populations on the spread of deliberate releases of infectious agents like smallpox.

1. Introduction

The study of the potential impact of epidemic outbreaks that arise from deliberate releases of biological agents became a "hot" topic of research after the events of September 11, 2001. Modeling techniques have been used to test the effectiveness of preventive or control measures on "worst case" scenarios (see for example, [**27, 13, 11, 9**]). In this paper, we will review recent efforts to model the role of public health interventions in models that account for individual behavioral changes or incorporate the impact of "transient" populations on the spread of deliberate releases of agents like smallpox. Results that may be useful in the identification of network-dependent effective intervention strategies are presented. After briefly reviewing the concepts and definitions associated with networks, we describe differences of epidemic patterns on small world, scale free and LLYD (Liu-Lai-Ye-Dasgupta) networks; next we consider the potential impact of a transient

1991 *Mathematics Subject Classification.* Primary 92D25, 92D30; Secondary 34B60, 05C80.
Key words and phrases. Mathematical epidemiology, differential equations, random networks, homeland security.
A. C.-A. and F. S. were partially funded by National Science Foundation under grant DMS-0441114, and National Security Agency under grant H98230-05-1-0097. B. S. was supported by FSIP of Montclair State University.

population on disease dynamics and the potential effects that individual behavioral changes may have on epidemic patterns in the case of smallpox.

2. Network models

One of the challenges in modeling transmission dynamics of diseases consists in finding adequate ways to incorporate the underlying contact structures into the model [**8, 4, 43, 24, 10**]. The nature of the contact network of individuals in a given population has, in some sense, become the primary engine behind the study of epidemics on networks and consequently, the use of particular network structures has received considerable attention [**40, 41**].
The mathematical study of graphs (networks) can be traced back to the 1960's work of Erdős and Rényi who devised a simple algorithm to generate random networks [**6**]. The algorithm begins with a fixed number of disconnected nodes N and then proceeds to connect (with an edge) with probability $p_{_{ER}}$ each pair of nodes independently. Hence, $p_{_{ER}} = 0$ corresponds to the case where no node is connected to any other $N-1$ nodes while $p_{_{ER}} = 1$ corresponds to the case where all nodes are connected to each other (complete graph). The total number of edges when $p_{_{ER}} = 1$ is $\binom{N}{2}$; the average number of edges is $\frac{N(N-1)p_{_{ER}}}{2}$; and, the average degree of a node (number of edges incident from a node) is $z = (N-1)p_{_{ER}} \simeq Np_{_{ER}}$ (for large N).

Erdős and Rény [**6**] showed that for large systems (large N) the probability that a node has k edges follows the Poisson distribution $P(k) = \frac{exp(-z)z^k}{k!}$, $(k = 0, 1, ..., N)$. They also identified a critical or threshold value (z_c) of z such that if $z > z_c$, then there is a *connected component* which is the subset of vertices that can be reached from all other vertices in this subset via some path through this subset of the network (the so called *spanning cluster* [**48**]). In the context of our work on epidemics in networks, the Erdős and Rényi random graph provides a null-model for the "comparative" study of the disease transmission on various networks. The case $p_{_{ER}} = 1$ (totally connected network) would be the generator of the networks most conducive to disease spread.

Watts and Strogatz (1998) [**49**] introduced a model of networks that interpolates between regular (lattices) and random networks. The Watts-Strogatz (WS) algorithm generates these networks by first constructing a one-dimensional periodic ring lattice of N nodes connected to its $2K$ nearest neighbors (K is known as the coordination number). Next, each edge is removed and "rewired" to a randomly selected node with probability $p_{_{WS}}$. That is, the WS algorithm shifts one end of the edge to a new randomly chosen node from the whole lattice with the constraint that no two nodes are allowed to have more than one edge running between them, and no node can be connected by an edge to itself. They classified their networks by level of randomness as measured by the disorder parameter $p_{_{WS}}$ (from "regular" $p_{_{WS}} = 0$ to completely random, $p_{_{WS}} = 1$). In the case of *regular* networks each node in the network is connected to its nearest K neighbors to the right and K neighbors to the left. Completely random WS networks are generated with $p_{_{WS}} = 1$. Watts and Strogatz showed that the introduction of a few random connections ($p_{_{WS}} \simeq 0.01$) significantly reduces the average distance between any two nodes (characteristic path length), a property that facilitates disease spread.

For small p_{WS}, Watts and Strogatz showed that the average distance between nodes grows like $O(log(N))$ and not as $O(N)$. Networks constructed by the WS algorithm have also high levels of clustering. These two characteristics (clustering and short average distance between nodes) describe the small-world effect, a phenomenon that has been detected in various networks including one of actors in Hollywood, the power generator network in the western US, and the neural network of *C.elegans* [**49**]. This "small-world effect" was documented earlier by the psychologist Stanley Milgram using data from the letter-passing experiments that he conducted in the 1960s [**36**]. Newman and Watts [**42**] studied a slight variation of this model that added shortcut edges with probability ϕ per edge in the underlying ring lattice instead of 're-wiring' the existing edges. The degree or connectivity distribution of small-world networks depends on the disorder parameter p_{WS}. In fact, when $p_{WS} = 0$, no re-wiring of edges occurs and hence a regular network is conserved. As p approaches 1, the connectivity distribution converges to that obtained from the Erdős and Rényi model.

The bell-shaped node degree distributions observed in the Erdős-Rényi, Watts-Strogtaz, and Newman-Watts models contrast with the highly right-skewed (power-law) degree distributions observed in a number of biological [**25**], social [**1, 2, 3, 38, 39, 32, 12**], and technological [**1, 2, 29, 17**] networks. Power-law degree distributions (also known as Pareto distributions by statisticians) are given by the parametric family:

$$P(k) = Ck^{-\alpha}$$

where $P(k)$ is the probability that a randomly selected node has degree k, α is typically between 2 and 3 (infinite variance), and C is a normalization constant such that the integral of $P(k)$ equals one. The degree of the nodes in a power-law network are distributed so that most nodes have only a few connections and a few nodes are highly connected. Barabási and Albert [**1**] dubbed these types of structures *scale-free* networks.

Liu, Lai, Ye, and Dasgupta (LLYD) [**33**] extended the Barabási-Albert model for scale-free networks by allowing new connections to be made uniformly at random to any other node in the network. Each new node connects to m existing nodes uniformly at random with probability p and following preferential attachment (higher probability of connecting to higher degree nodes) with probability $1 - p$. Large LLYD networks [**33**] have a degree distribution $P(k) \sim k^{-c}$ (Scale-Free) as $p \to 0$ whereas $P(k) \sim e^{-k/m}$ (Erdös-Rényi) as $p \to 1$.

2.1. Epidemics on networks. Stochastic epidemic models on networks can be used to assess the role of contact structures in the progression of epidemics where the nodes represent individuals in the population. There is an edge between two nodes if the individuals represented by the nodes have contact with each other that could spread the disease. Moore and Newman [**37**] studied SIR (susceptible-infected-recovered) epidemics on small world networks via site and bond percolation. In the simplest setting, individuals/nodes of the network can be in one of three epidemiological states: susceptible, infectious, and recovered (SIR). A susceptible individual in contact with i infectious individuals may become infected in a short period of time δt with a probability given by $\beta i \delta t$ where β is the constant risk of infection per unit of time and $\delta t = 1$ in this discrete time model. Similarly,

infected individuals recover with a probability given by $\gamma\delta t$ where $\frac{1}{\gamma}$ is the mean period of infectivity. Recovered individuals are immune to the disease.

Pastor-Satorras and Vespignani [**45**] studied an SIS epidemic model where recovered individuals are still susceptible to future infections on scale-free networks (generated using the BA model). They found that the disease may persist independently of its transmissibility. An SIR process on scale-free networks leads to similar conclusions (May and Lloyd [**34**]). Pastor-Satorras and Vespignani [**46**] and independently Dezso and Barabási [**14**] concluded that immunization campaigns targeted towards the most connected nodes or hubs increase the probability of recovering finite epidemic threshold behavior. However, May and Lloyd [**34**] showed that in finite size networks, infections cannot spread for arbitrarily low transmission probabilities. A contrasting result has been established on highly clustered scale-free networks [**28**] where a finite epidemic threshold can be recovered using an SIS epidemic model (Eguíluz and Klemrn [**16**]).

We study the effect of interventions aiming at lowering the transmission rate by reducing the susceptibility of the population (e.g., increase hygiene, use of protective devices, vaccination) or from infectious individuals taking precautions that limit or reduce transmission to others. Thus, we explore the impact of decay in the transmission rate from b_1 to b_2 (that is, $b_2 < b_1$), a decrease that begins at the intervention time τ. Hence, the time dependent transmission rate used in our simulations is given by:

$$\beta(t) = \begin{cases} b_1 & \text{if } t < \tau \\ \\ b_2 & \text{if } t \geq \tau \end{cases} \tag{2.1}$$

where $0 < b_2 < b_1$.

In what follows we explore the role of these interventions in reducing the final size of epidemics in small-world and LLYD networks.

2.1.1. *Epidemics without interventions.* Figure 1 shows the mean final epidemic size as a function of the transmission rate β. It is clear that for small values of the transmission rate β, the mean final epidemic size is quite small. On the other hand, for larger values of β, most of the nodes became infected during typical simulated outbreaks. The simulated outbreaks corresponding to Figure 1 have an epidemic threshold (scale-free network of finite size [**34**]). For homogeneous mixing populations, the contact number (or basic reproductive number) is the average number of secondary infections generated by an infectious case during its infectious period in a completely susceptible population.The contact number is defined by $R_0 = \beta/\gamma$, as the product of the transmission rate β and the average length of the infectious period $1/\gamma$ [**23**]. In homogeneous mixing populations, if $R_0 > 1$ an epidemic will spread. Yet in the LLYD networks the threshold condition does not happen at $R_0 = 1$.

Figure 2(a) shows the mean final epidemic size, as a function of the network architecture (disorder parameter p). For each fixed value of p, the average of 50 realizations of the simulated outbreaks is depicted for $R_0 = \beta/\gamma = 2$. Five nodes were employed as *epidemic seeds* and chosen from the network uniformly at random (dashed), and by the highest degree (solid). The *epidemic seeds* have no significant

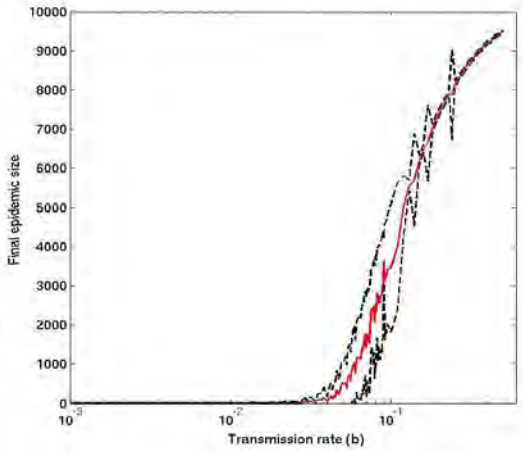

FIGURE 1. Mean final epidemic size as a function of the transmission rate β for scale-free networks (Barabási-Albert) of size 10^4. The recovery rate was set to $\gamma = 2/7$ and, five initial infected nodes were chosen uniformly at random. The mean (solid) of 50 realizations and 95% confidence intervals (dashed) are shown.

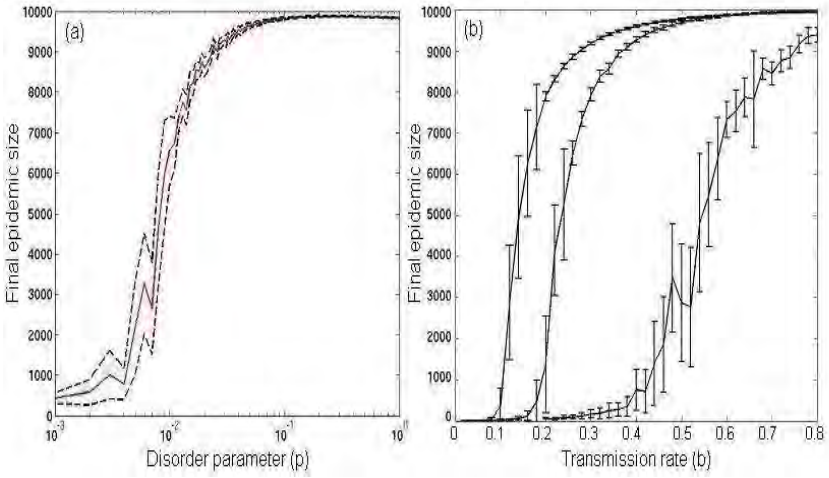

FIGURE 2. The mean final epidemic size for small-world networks with 10^4 nodes and $\langle k \rangle = 4$ with $\beta/\gamma = 2$ as a function of (a) the network disorder parameter p where the dashed line is the result of placing the five initial infectious nodes uniformly at random versus placing them in the highest degree nodes (solid), and (b) as a function of the transmission rate for three different levels of disorder p=1, 0.1, 0.01 (curves from left to right).

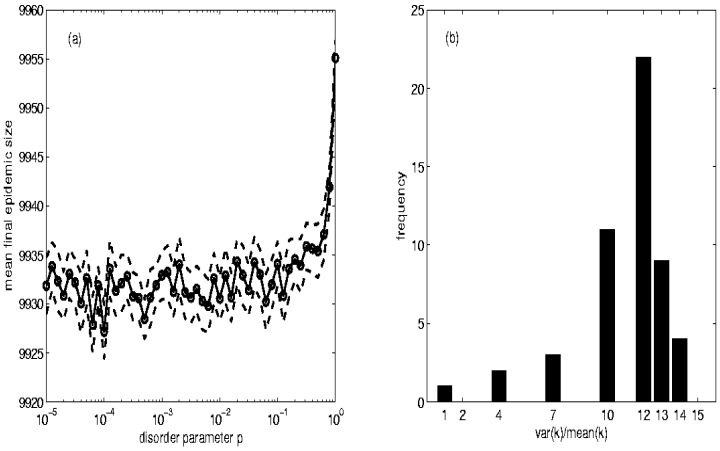

FIGURE 3. (a) The mean final epidemic size of 50 realizations (circle-solid) and 95% confidence intervals (dashed) for LLYD networks with 10^4 nodes and $m = 3$, where $\beta/\gamma = 2$, and 5 initial infected nodes chosen uniformly at random. (b) Ratios of variance to mean of the connectivity distributions for the LLYD networks used in (a).

effect on the size of outbreaks except for small values of the disorder parameter (architectures nearly regular, $p \in [10^{-3}, 10^{-2}]$) .

In Figure 2(b) the mean final epidemic size is displayed as a function of the transmission rate, for three values of the disorder parameter, $p = 0.01$, $p = 0.1$, and $p = 1$. The location of the sharp epidemic threshold occurs for smaller transmission rates as the disorder parameter increases.

In Figure 3, we show results obtained from simulations in LLYD networks. For LLYD networks, the tuning parameter p, weights the preferential attachment and uniform connections in the network growth model. Increments in p do not affect the average distance between nodes of the stochastically drawn networks [**30**] unlike small world networks.

The characteristic path length of LLYD networks as $p \to 0$ remains low because the hubs (nodes with high number of edges) act as long-range connections across the networks. Networks with short characteristic paths have large contact numbers. That is, network architectures as $p \to 0$, with short characteristic paths still favor epidemic spread. Furthermore, since the navigability is not perturbed across all increments in p, then such optimal spread quality is propagated through the entire family of LLYD networks. In Figure 3(a), we see that all the simulated outbreaks (across the LLYD networks) yielded mean final epidemic sizes above 99% of the total population. In Figure 3(b), we observe that, for those LLYD networks used in the stochastic simulations summarized in Figure 3 (a), most networks (over 85%) report having $10 < \frac{\langle k^2 \rangle}{\langle k \rangle} < 15$.

2.1.2. *Epidemics with delayed interventions.* Now we investigate how intervention times affect the mean final epidemic size across several network models.

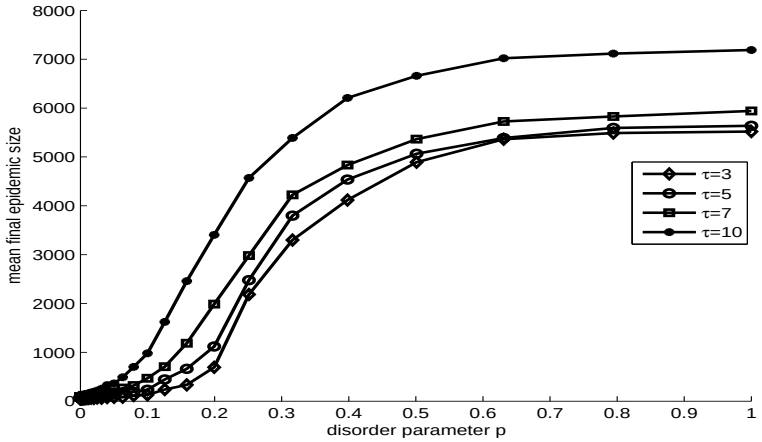

FIGURE 4. Mean final epidemic size as a function of the disorder parameter p for small-world networks of size 10^4 nodes with $\langle k \rangle = 4$ for various intervention times τ. The fastest intervention, $\tau = 3$, gives the smallest mean final epidemic size providing a reduction of about 50% with respect to the final epidemic size without interventions.

Several simulations were carried out for specific values of the intervention time $\tau \in \{3, 5, 7, 10\}$. The recovery rate was set to $\gamma = 2/7$, and assumed that interventions were capable of reducing transmission by 75%. Hence, the transmission rate was set to,

$$\beta(t) = \begin{cases} 4/7 & \text{if } t < \tau \\ 0.25 \times 4/7 & \text{if } t \geq \tau \end{cases} \tag{2.2}$$

In Figure 4 we show simulation results obtained on small-world networks. The average (of 50 realizations) is plotted as a function of the networks disorder parameter p, for several intervention times τ. The average epidemic sizes undergo a sharp transition as in our results without interventions. Figure 4 shows that there is a gradual increase in the mean final epidemic size, as the intervention time increases. Indeed, the fastest intervention time, $\tau = 3$, yielded an approximate average reduction in the final epidemic size of 50%.

For LLYD networks with interventions, the mean final epidemic size is shown in Figure 5 as a function of the networks' growth parameter p. Note that the effect of interventions on the final epidemic size is not as significant as in small-world networks. This can be explained by the presence of highly connected nodes in LLYD networks. Figure 5 shows that the fastest intervention time, $\tau = 3$, reduces the average final size by 5%, compared to Figure 3(a).

3. Potential Deliberate Release in Mass Transportation Systems

Smallpox is a viral communicable disease that can be passed from person to person by the inhalation of air droplets, from aerosols expelled from the oropharynx of infected persons, or by direct contact with infectious individuals. Transmission

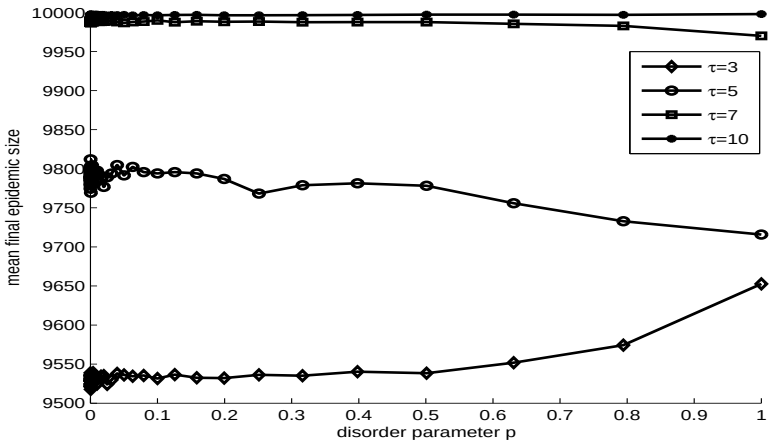

FIGURE 5. The effect of intervention times on the final epidemic size for LLYD networks of size 10^4 with $m = 5$. The reductions in the final epidemic size due to interventions are not as significant as for small-world networks.

is more likely whenever susceptible individuals are within a seven-foot radius from an infectious person (long-distance airborne transmission is possible [**7, 26, 50**]). Exposure, is followed by an incubation (latent/exposed) period lasting between 7 and 17 days (the mean duration is between 12 and 14 days). During the incubation period, individuals do not show symptoms and do not feel "sick". However, twelve to fourteen days after infection, infected individuals become febrile, have severe aching pains, high fever, and often must stay in bed (prodrome phase). Infected persons are most contagious two to three days following the prodrome state, the period of infectiousness lasts about four days. Afterwards, a rash develops over the face that spreads to the extremities. This rash soon becomes vesicular and later, pustular. The patient remains febrile throughout the evolution of the rash and tends to experience considerable pain as the pustules grow and expand. Gradually, scabs form, which leave pitted scars after separation. When death happens, it usually occurs during the second week [**21**].

Smallpox and anthrax are two of the most likely biological agents to be used in a deliberate release [**47**] since they are easily aerosolized and support high case fatality rates. The earliest mathematical smallpox epidemic model is attributed to Daniel Bernoulli [**5**]. His goal was to calculate the adjusted life table when smallpox was eliminated as a cause of death [**15**]. Interest on homeland security issues have resulted in the development of a series of models geared towards the exploration of the consequences of the use of smallpox as a biological agent [**20, 22, 27, 35**].

Potential smallpox release targets include mass transportation systems, airport hubs, or terminals within major metropolitan areas. Here, we use New York City (NYC) with a population of about 8 million that includes 4.3 million subway users during weekdays alone, to develop our mathematical model [**9**]. The city or metropolitan area under consideration is divided into N neighborhoods and multiple levels of mixing between individuals are introduced. The population is subdivided

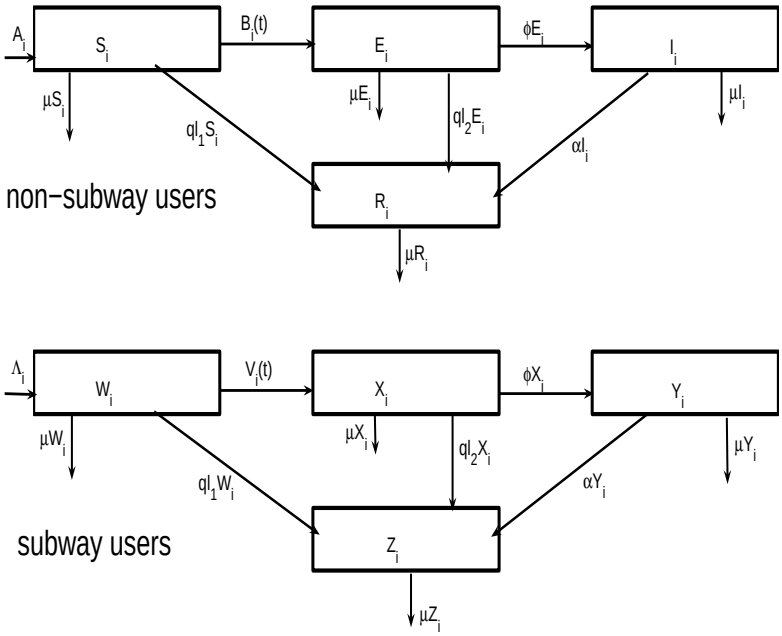

FIGURE 6. Diagram for the transmission of smallpox in one neighborhood. The mixing between users and non users within the same neighborhood is formulated by $B_i(t)$ and the users among different neighborhoods by $V_i(t)$.

into "subway" or "mass transportation" users (SU) and non-subway or non public transportation users (NSU). SU-individuals may have contacts with SU and NSU individuals in their *own* neighborhoods as well as contacts with SU-individuals from other neighborhoods when they share a ride in a mass transportation system. To simplify our model, we assume that contacts between SU individuals from different neighborhoods outside the mass-transportation system are rare (for the purpose of disease transmission) and are ignored. We further assume that NSU-individuals have *all* of the contacts that could lead to disease transmission within their own neighborhood.

We proceed with the typical simulation by introducing a fixed number of infected individuals in the public transportation system and proceed to follow the patterns of disease spread. Newly infected individuals take the virus back to their own neighborhoods generating infections in the NSU and SU populations. Once the attack is recognized and smallpox is detected, mitigation policies, such as vaccination begin. We will use the model to quantify the impact of *delays* in detection or response to the epidemic.

We classify individuals into one of four epidemiological classes within each neighborhood. We define S_i, E_i, I_i, and R_i to be the numbers of NSU in neighborhood i who are susceptible, exposed, infectious, and recovered, respectively and W_i, X_i, Y_i, and Z_i the corresponding epidemiological classes for SU individuals within the same neighborhood. The total population sizes of the two groups are given by $Q_i = S_i + E_i + I_i + R_i$ and $T_i = W_i + X_i + Y_i + Z_i$. We proceed to define appropriate multilevel mixing structures and this, as we shall see, cannot be done arbitrarily. Mixing patterns are a function of individual activity levels and population size or frequency ([**8, 10**]). Hence, we let the constants a_i and b_i be the per-capita contact rates of NSU and SU individuals of neighborhood i. Furthermore, we let $\omega_i = \rho_i/(\sigma_i + \rho_i)$ and $\tau_i = \sigma_i/(\sigma_i + \rho_i)$ where ρ_i and σ_i be the rates at which the SUs get on and off the subway. Hence, ω_i and τ_i represent the fractions of "contact time" that a typical SU-individual spends on or off the subway, respectively. Following the standard modeling approach for the contact structure between various individuals, but now restricted to a *particular* mixing level, we assume the proportional mixing between the population groups [**4, 8, 43, 24**]. The proportional mixing "probabilities" are given in Table 1.

Mixing probability	Individuals of mixing
$\tilde{P}_{a_i} = \frac{a_i Q_i}{a_i Q_i + b_i \tau_i T_i}$	NUS of the same neighborhood i.
$\tilde{P}_{b_i} = \frac{b_i \tau_i T_i}{a_i Q_i + b_i \tau_i T_i}$	NSU and US of the same neighborhood i.
$\bar{P}_{a_i} = \frac{a_i Q_i}{a_i Q_i + b_i \tau_i T_i} \tau_i$	US and NUS of the same neighborhood i.
$\bar{P}_{b_i} = \frac{b_i \tau_i T_i}{a_i Q_i + b_i \tau_i T_i} \tau_i$	US from the same neighborhood i.
$\bar{P}_{b_j^i} = \frac{b_j \omega_j T_j}{\sum_{k=1}^{N} b_k \omega_k T_k} \omega_i$	US from neighborhoods i and j.
$P_{a_i a_j} = 0 \ (i \neq j)$	NUS of neighborhoods i and j .
$P_{a_i b_j} = 0 \ (i \neq j)$	NSU of neighborhood i and US of neighborhood j.

TABLE 1. Formulas for mixing probabilities.

As it was noted, these mixing proportions cannot be arbitrarily defined and in fact, it can be checked that for each neighborhood the following two *"conditional probability"* identities hold:

$$\tilde{P}_{a_i} + \tilde{P}_{b_i} = 1, \quad i = 1, 2, ..., N. \tag{3.1}$$

$$\bar{P}_{a_i} + \bar{P}_{b_i} + \sum_{j=1}^{N} \bar{P}_{b_j} = \tau_i + \omega_i = 1, \quad i = 1, 2, ..., N. \tag{3.2}$$

Figure 6 schematically describes the movement of people of different type and different epidemiological status for a typical neighborhood.

The model equations first introduced in ref. [**9**] are:

$$\frac{dW_i}{dt} = \Lambda_i - V_i(t) - (\mu + q_i l_1)\, W_i, \tag{3.3}$$

$$\frac{dX_i}{dt} = V_i(t) - (\mu + \phi + q_i l_2)\, X_i, \tag{3.4}$$

$$\frac{dY_i}{dt} = \phi X_i - (\mu + \alpha + d)\, Y_i, \tag{3.5}$$

$$\frac{dZ_i}{dt} = \alpha Y_i - \mu Z_i + q_i l_1 W_i + q_i l_2 X_i, \tag{3.6}$$

$$\frac{dS_i}{dt} = A_i - B_i(t) - (\mu + q_i l_1)\, S_i, \tag{3.7}$$

$$\frac{dE_i}{dt} = B_i(t) - (\mu + \phi + q_i l_2)\, E_i, \tag{3.8}$$

$$\frac{dI_i}{dt} = \phi E_i - (\mu + \alpha + d)\, I_i, \tag{3.9}$$

$$\frac{dR_i}{dt} = \alpha I_i - \mu R_i + q_i l_1 S_i + q_i l_2 E_i, i = 1, ..., N, \tag{3.10}$$

where the infection rate for those who do not use mass transportation is

$$B_i(t) = \beta_i a_i S_i \left(\tilde{P}_{a_i} \frac{I_i}{T_i \tau_i + Q_i} + \tilde{P}_{b_i} \frac{Y_i \tau_i}{T_i \tau_i + Q_i} \right), \tag{3.11}$$

and the infection rate for mass transportation users is

$$V_i(t) = \beta_i b_i W_i \left(\bar{P}_{a_i} \frac{I_i}{T_i \tau_i + Q_i} + \bar{P}_{b_i} \frac{Y_i \tau_i}{T_i \tau_i + Q_i} + \sum_{j=1}^{N} \bar{P}_{b_j^i} \frac{Y_j \omega_j}{T_j \omega_j} \right) \tag{3.12}$$

with

$$Q_i(t) = S_i(t) + E_i(t) + I_i(t) + R_i(t),$$
$$T_i(t) = W_i(t) + X_i(t) + Y_i(t) + Z_i(t).$$

The multilevel mixing possibilities complicate the expressions for the incidence rates in Equation 3.12. Parameters are defined in Table 2.

The proportionate mixing ([**8, 4, 43, 24**]) is used. Suppose, in general, that there are two types of individuals. The probability that a type 1 individual has a contact with type 2 individual, given that the type 1 individual has had a contact, is equal to the *weighted* proportion of type 2 individuals activity in the total population (that is, it is independent of type 1 individuals). Because SU individuals do not spend their entire time in their "home" neighborhood, some modifications are required. Here, we deal with this by assuming proportional budgeting of SU contacts. For example, $\tilde{P}_{a_i} = \frac{a_i Q_i}{a_i Q_i + b_i \tau_i T_i}$ computes the mixing probability between non-subway users from the same neighborhood i. The numerator $a_i Q_i$ is the average activity of NSU while the denominator $a_i Q_i + b_i \tau_i T_i$ gives the average total activities in neighborhood i, noticing that SU within neighborhood activity has to be weighted by the additional factor τ_i.

Parameters	Definitions
Λ_i	Recruitment rate of subway users
A_i	Recruitment rate of non-subway users
μ	Natural mortality rate
d	Mortality rate due to smallpox
q_i	Per capita vaccination rate
l_1, l_2	Vaccination efficacy in susceptible and exposed populations
ϕ	Progression rate from latent to infectious
α	Recovery rate
σ_i	The rate at which an SU leaves the subway
ρ_i	The rate at which an SU gets in the subway
a_i	Average number of contacts of NSU per unit of time
b_i	Average number of contacts of SU per unit of time
β_i	Transmission rate per contact
$\frac{1}{\rho_i}$	The average time spent on the subway
$\frac{\sigma_i}{\sigma_i+\rho_i}$	The proportion of time spent off the subway (SU)
$\frac{\rho_i}{\sigma_i+\rho_i}$	The proportion of time spent on the subway (SU)

TABLE 2. Definitions of parameters. Here, i is the index of a neighborhood.

As it was done in ref. [**9**], we apply the above model to a city like New York City. We consider a highly simplified situation such that we stratify the population into only two "neighborhoods." The first includes regular residents while the second consists of temporary residents (such as tourists). Parameters that are somewhat consistent with the situation in NYC are estimated and listed in Table 3 (The rationale behind parameter selection can be found in [**9**]). The selections of $\tau_1 = 0.6$ and $\tau_2 = 0.1$ follow from the assumption that non-residents spend considerably more time on mass transportation than residents. Residents are assumed to spend most of their time in their own neighborhood, that is, not within the mass transportation system.

μ	d	l_1	l_2	ϕ	α	β	a_1	a_2	b_1	b_2
0.033	0.0116	0.97	0.3	0.086	0.086	0.5	5	10	15	30

TABLE 3. Parameter values

It is assumed that smallpox is released in the subway system and that initially $Y_1(0)$ and $Y_2(0)$ are positive. Furthermore, we let $Y_1(0) = 70$ and $Y_2(0) = 30$ (that is, there are 100 persons infected initially on the subway). The initial values of W_1, S_1, W_2 and S_2 are chosen to satisfy $W_1(0)+S_1(0) = 8,000,000$ and $W_2(0)+S_2(0) = 200,000$. The rest of initial values are set to zero, that is, $I_1(0) = I_2(0) = X_1(0) = X_2(0) = Z_1(0) = Z_2(0) = R_1(0) = R_2(0) = 0$.

The impact of varying the parameters q_1 and q_2 and the vaccination rates for the resident population and tourist populations are then explored. Specifically, the impact of varying q_1 and q_2 on the basic reproductive number, R_0, is explored visually. Figure 7 gives a plot of $R_0(q_1, q_2)$ as a function of q_1 and q_2. The regions where $R_0(q_1, q_2) < 1$, $R_0(q_1, q_2) = 1$ and $R_0(q_1, q_2) > 1$ are also marked in the same figure. We note that the vaccination rate for the resident population needs

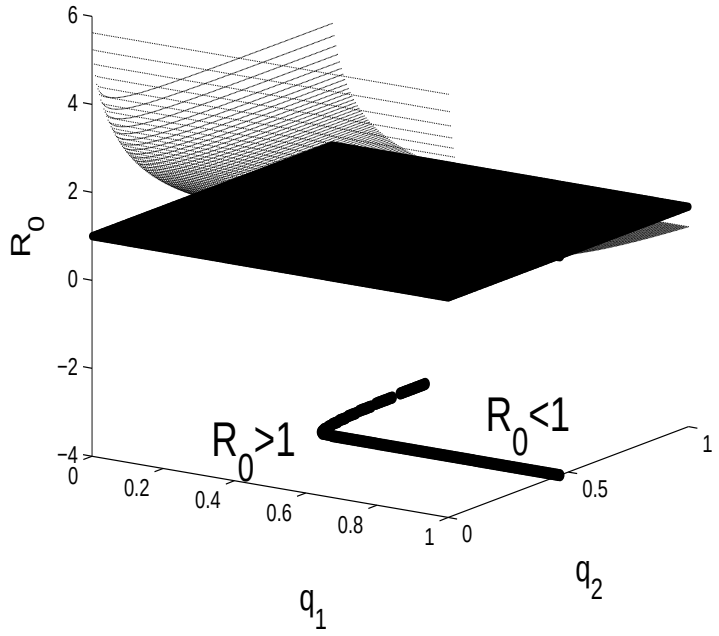

FIGURE 7. Plot R_0 versus q_1 and q_2 and control region on the (q_1, q_2)-plane.

to be greater than 0.46 and that the impact of the nonresident population is less important (*for a city outbreak*) but *not* irrelevant (its vaccination rate could be as low as 0.26). Preliminary simulations have supported mass vaccination (MV) as the "best" strategy for NYC. It was seen that the last smallpox outbreak in NYC in 1947 was caused by 8 cases, but it ended with 6 million people vaccinated (almost complete coverage)[**18**]. Our initial introduction of 100 infections may or may not be consistent with a deliberate release (we have no data). Model simulations in the above scenario agree with R. Larsen's recommendations, but only in the event of a large-scale outbreak [**31**].

Delays in the implementation of a control policy like vaccination lead to quite distinct scenarios. When everybody is vaccinated as soon as the first infected is detected, then only 27 people die as a result of this release under MV (see Figure 8).

Not surprisingly, response time plays a critical role whenever the goal is to reduce the total number of deaths. Figure 8 compares the number of cases and total deaths in situations where there is an immediate response, a one-day delay, a two-day delay, and a three-day delay. As can be seen from Figure 8, a one-day delay results in 26 additional deaths and 100 more cases even if 80% of the total population is vaccinated ($q_1 = q_2 = 0.8$) on the second day. A two-day delay in the vaccine implementation results in (66 more deaths) with 131 additional deaths

if vaccination were to start 3 days later. Figure 8 also shows the appearance of a second wave about 8 days after the initial release of smallpox on the public transportation system despite the vaccination policy.

From these simulations and as specified in [**9**] delays in response to an attack (vaccination implementation) and exclusive emphasis on the resident population may result in serious consequences (but see the next section). Hence, the development of effective surveillance systems is critical.

4. Effects of Behavioral Changes during a Deliberate Release of Smallpox

Concern that smallpox could be used as a biological weapon has prompted scientists and government officials to prepare emergency response plans in the event of a deliberate or accidental release. The smallpox response policy of the Center for Disease Control and Prevention (CDC) includes the statement, "Any vaccination strategy for containing a smallpox outbreak should use the ring vaccination concept. This includes isolation of confirmed and suspected smallpox cases with tracing, vaccination, and close surveillance of contacts to these cases as well as vaccination of the household contacts of the contacts" [**51**]. However, CDC's policy does not explicitly take into account the impact of individuals' decisions to change their behavior.

In addition to the public health interventions mentioned above, changes in behavior in the affected population in response to a smallpox attack are expected. For example, people could decide to wash their hands more frequently, wear protective masks, and avoid crowded places; people could stay home from work; and businesses could close. It is surprising that the likely occurrence of these behavior changes has not been included explicitly in previous computer simulations of

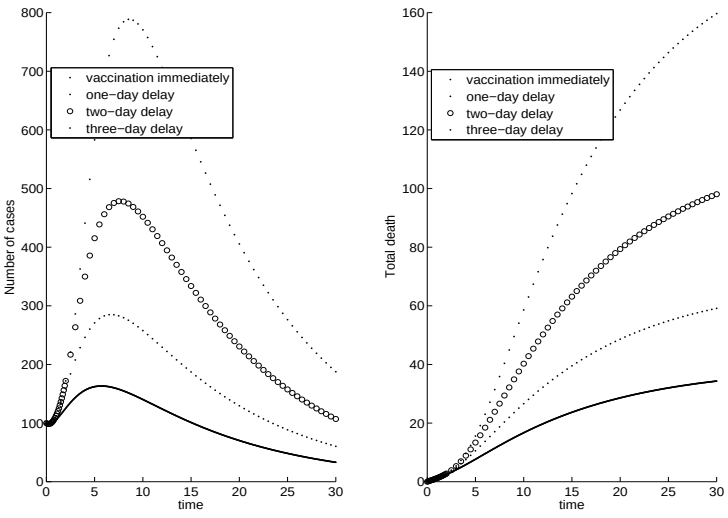

FIGURE 8. Total deaths and cases for different response times.

a smallpox epidemic [**9, 19, 27, 35**]. Without including behavioral changes, the simulations predict unrealistic "worst" case scenarios. Recent experiences with the SARS epidemics show that an outbreak of a deadly disease like smallpox would generate dramatic behavioral changes [**44**].

To assess the impact of individual and community behavioral changes in response to a disease with high mortality, we divide the population in two groups: the normally active group (subscript n) and the less active group (subscript ℓ). We assume that individuals in the less active group reduce their average number of contacts in response to information about smallpox cases in the community. Individuals in each activity group ($j = n$ or ℓ) are characterized by their epidemiological status as: susceptibles, exposed, infectious, vaccinated, quarantined, isolated, recovered, or dead. The transfers between epidemiological compartments are shown diagrammatically in Figure 9.

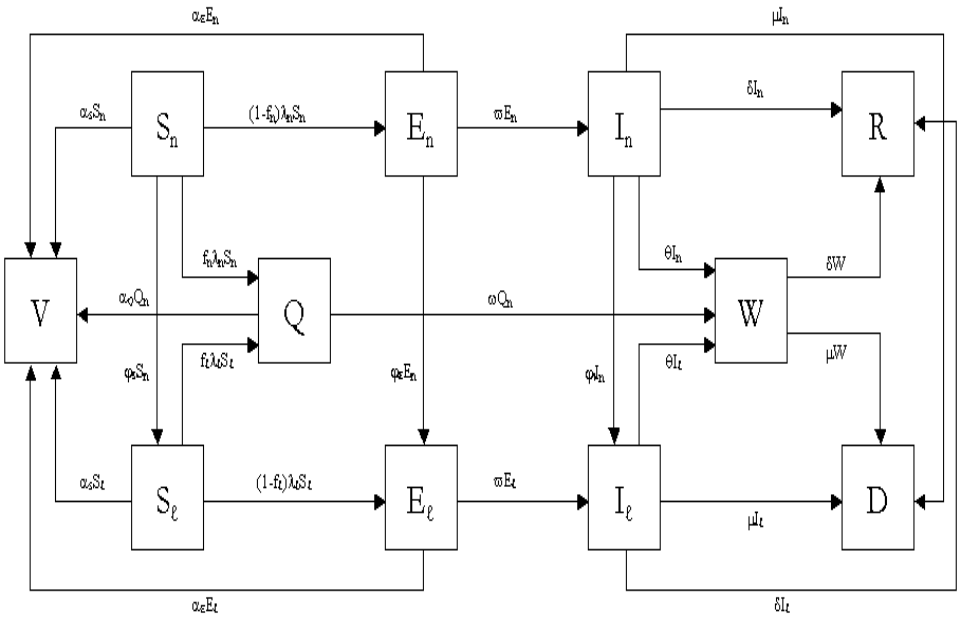

FIGURE 9. Schematic relationship between normally active and less active individuals ($j = n, \ell$) for smallpox infection. The arrows that connect the boxed groups represent movement of individuals from one group to an adjacent one. Susceptible individuals (S_j) can become exposed (E_j), be quarantined (Q) or vaccinated (V). Exposed individuals can either become infectious (I_j) after an incubation period or be vaccinated. Quarantined individuals can either be vaccinated or isolated (W). Infectious individuals can be isolated or can either recover (R) or die (D). Similarly, isolated individuals can either recover or die.

Using the transfer diagram in Figure 9, we arrive at the following nonlinear system of differential equations:

$$
\begin{aligned}
\dot{V} &= \alpha_S(S_n + S_\ell) + \alpha_E(E_n + E_\ell) + \alpha_Q Q, \\
\dot{S}_n &= -\lambda_n S_n - (\varphi_S + \alpha_S)S_n, \qquad \lambda_n = \gamma_n \beta \left(\frac{\gamma_n I_n + \gamma_\ell I_\ell + \gamma_c W}{\gamma_n A_n + \gamma_\ell A_\ell + \gamma_c A_c} \right), \\
\dot{S}_\ell &= -\lambda_\ell S_\ell + \varphi_S S_n - \alpha_S S_\ell, \qquad \lambda_\ell = \gamma_\ell \beta \left(\frac{\gamma_n I_n + \gamma_\ell I_\ell + \gamma_c W}{\gamma_n A_n + \gamma_\ell A_\ell + \gamma_c A_c} \right), \\
\dot{Q} &= f_n \lambda_n S_n + f_\ell \lambda_\ell S_\ell - (\omega + \alpha_Q)Q, \\
\dot{E}_n &= (1 - f_n)\lambda_n S_n - (\varphi_E + \omega + \alpha_E)E_n, \\
\dot{E}_\ell &= (1 - f_\ell)\lambda_\ell S_\ell + \varphi_E E_n - (\omega + \alpha_E)E_\ell, \\
\dot{I}_n &= \omega E_n - (\varphi_I + \mu + \delta + \theta)I_n, \\
\dot{I}_\ell &= \omega E_\ell + \varphi_I I_n - (\mu + \delta + \theta)I_\ell, \\
\dot{W} &= \theta(I_n + I_\ell) + \omega Q - (\mu + \delta)W, \\
\dot{R} &= \delta(I_n + I_\ell + W), \\
\dot{D} &= \mu(I_n + I_\ell + W).
\end{aligned} \tag{4.1}
$$

Parameter definitions are summarized in Table 4.

Parameter	Description	Dimension	Baseline
$\Re_{unc}$	Basic Reproductive Number	1	3
δ	Recovery relative rate	Day^{-1}	$(16)^{-1}$
θ	Isolation relative rate	Day^{-1}	$(5)^{-1}$
μ	Death relative rate	Day^{-1}	0.0267
ω	Incubation relative rate	Day^{-1}	$(15)^{-1}$
α_S	Vaccination relative rate for susceptibles	Day^{-1}	0.01
α_E	Vaccination relative rate for exposed	Day^{-1}	0.015
α_Q	Vaccination relative rate for quarantined	Day^{-1}	0.0167
φ_S	S_n behavior change relative rate	Day^{-1}	0.076
φ_E	E_n behavior change relative rate	Day^{-1}	0.082
φ_I	I_n behavior change relative rate	Day^{-1}	0.089
f_n	Fraction of S_n found by contact tracing	1	0.8
f_ℓ	Fraction of S_ℓ found by contact tracing	1	0.8

TABLE 4. Parameter definitions and values that fit the cumulative number of cases for the model.

We carried out numerical simulations and assumed that 0.001% infected individuals in a population of 1 million people enter the incubation phase after being successfully infected during a smallpox attack. The standard intervention procedures for smallpox control are isolation, quarantine, ring vaccination, and mass vaccination. Another factor that would affect the extent and duration of a smallpox epidemic is the reduction in contacts of people in response to information about the smallpox epidemic. Based on the extensive behavioral changes that occurred during the SARS outbreaks, it is clear that similar reductions in contact rates would also occur after the deliberate release of a biological agent such as smallpox. In ref. [**13**], we used a computer simulation model to examine the effects on the

epidemic after a smallpox attack of the standard smallpox interventions combined with behavioral change in the population. Although the changes in behavior in our simulations are gradual and moderate, they have a dramatic impact on the size and length of the smallpox epidemic.

For single intervention strategies, we assumed that all interventions start 20 days later. Estimates on the transmission of smallpox indicate that 1 infected person may infect 3 to 6 others. Therefore, the basic reproductive number was set to 3. The baseline scenario shows that almost everyone in the population is infected with smallpox in the absence of interventions. Figure 10 shows that with isolation only, the epidemic decays very slowly with 296 smallpox cases at 365 days. When only quarantine is used, the total cumulative smallpox cases is lower, at 223. Ring vaccination of quarantined people, leads to slightly fewer total smallpox cases. With high behavioral change there are only 108 total smallpox cases. Mass vaccination (see [**13**]) leads to a total of 1640 smallpox cases, which is much higher than any other intervention.

For combined intervention strategies, we assume that all interventions start 20 days after the initially infected people enter the incubation phase. In Table 5 the strategy of isolation combined with ring vaccination and mass vaccination is quite effective with only 50 total smallpox cases. With high behavioral change the total smallpox cases decreases to 40, and the epidemic is shorter. Results with medium and low behavioral change have slightly more smallpox cases and slightly longer epidemics.

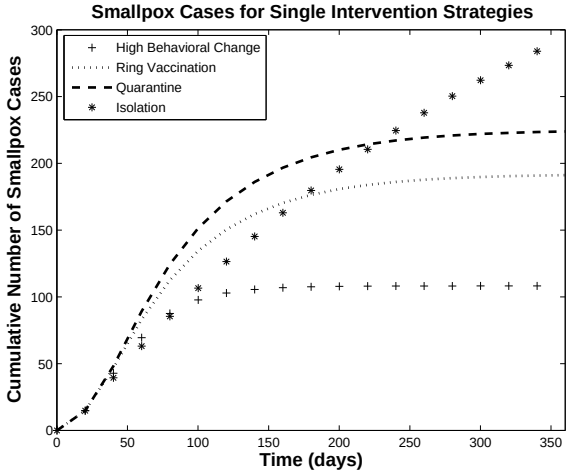

FIGURE 10. Cumulative number of smallpox cases for various single intervention strategies. An intervention of high behavioral change only leads to 108 total smallpox cases (+) while ring vaccination only leads to 191 total smallpox cases (:). A quarantine only strategy leads to 223 total smallpox cases (−−) and isolation only leads to 296 total smallpox cases (∗).

The numerical simulation results show that without any interventions, almost everyone is infected by the final day. This is not surprising, since with an

TABLE 5. Estimates of cumulative total of smallpox cases for combination intervention strategies.

Intervention	60 days	180 days	365 days	Final day[a]
Isolation, RV* & MV*	**45**	**50**	**50**	98
Isolation, RV, MV & HBC*	**38**	**40**	**40**	81
Isolation, RV, MV & MBC*	**40**	**42**	**42**	83
Isolation, RV, MV & LBC*	**42**	**44**	**44**	86

[a] Days from infection of index cases until outbreak is controlled (when the number of cases reaches 99% of the final epidemic size).

* Ring Vaccination (RV), Mass Vaccination (MV), High Behavioral Changes (HBC), Medium Behavioral Changes (MBC), and Low Behavioral Changes (LBC).

uncontrolled reproduction number of 3, the initial growth is exponential. In the simulations, behavioral changes without any other interventions were able to control the epidemic. In other words, the behavioral change intervention was more effective than any other single intervention. All strategies in Table 5 with mass vaccination do yield shorter outbreaks with fewer total smallpox cases than the same strategies without mass vaccination. Hence, the addition of mass vaccination does lead to slightly better results, but the small improvements are probably not worth the cost of vaccinating so many people. Our simulations show that following a smallpox release, mass vaccination is the least effective strategy, when cost and logistic difficulties are considered.

Although the parameter values were estimated from epidemiological data, we explored the sensitivity to various components of the model, including the effects of changes in $\Re_0$, delays in implementing intervention strategies, and the number of initially exposed individuals (see ref. [**13**] for details). We found that the simulation results are most sensitive to the uncertainty associated with $\Re_0$, the time at which intervention start, the number of index cases, and the isolation rate.

We conclude that for simulations of a smallpox outbreak to be useful in guiding public health policy, they must consider the impact of behavioral changes. Policies regarding recommendations on behavioral changes need planning, before they can become part of the smallpox response plan. The qualitative conclusions reached here are useful in providing estimates of the effects of behavioral changes.

5. Concluding Remarks

The research reported in this paper is motivated by concerns about the potential impact of deliberate releases of biological agents and our nation's readiness to limit the consequences of such a disaster. Do we have the appropriate framework in which we can explore the consequences of events for which we have no data? In order to highlight the importance and relevance of stochastic approaches in this context, we address questions of interest using two approaches: stochastic epidemics in networks and deterministic "classical" epidemics. The fact that each approach is best suited for specific questions becomes immediately evident and the need to use both (and other approaches) is overwhelmingly clear. Deterministic epidemic models can indeed incorporate dynamic network structures that account for changes in population size and behavior modification in a *tractable* manner while network

epidemic models are extremely useful in identifying in a probabilistic sense the role of divergent contact structures on disease patterns–including the final epidemic size.

Acknowledgements

We thank Alun Lloyd, Ying-Cheng Lai, and Cindy Greenwood for stimulating conversations. A. C.-A. acknowledges financial support from the Department of Mathematics and Statistics of Arizona State University. F. S. acknowledges financial support from the Alfred P. Sloan Foundation and Cornell University.

References

[1] Barabási, A.-L. and Albert, R. *Emergence of Scaling in Random Networks*, Science **286**, 509-512 (1999).

[2] Barabási, A.-L., Albert, R., Jeong, H. *Mean-field theory for scale-free random networks*, PHYSICA A **272**, 173-87 (1999).

[3] Barabási, A.-L., Jeong, H., Ravasz, R., Z. Nda, T. Vicsek,and A. Schubert, *On the topology of the scientific collaboration networks*, Physica A **311**, 590-614 (2002).

[4] Barbour, A.D. Macdonal's model and the transmission of bilharzia, *Trans, Roy. Trop. Med. Hyg.*, **72**, 6-15 (1978).

[5] Bernoulli, D., Mém. Math. Phys. Acad. R. Sci. Paris 145, 1766; English translation and translation and critical commentary by L. Bradley in Smallpox Inoculation: An Eighteenth Century Mathematical Controversy (Adult Education Department, Nottingham, 1971).

[6] Bollobás, B. *Random Graphs* (1985) (Academic, London).

[7] Broad W.J., and Miller, J. Report provides new details of Soviet smallpox accident, *the New York Times*, June 15, 2002, sect. A, pp. 1.

[8] Busenberg, S. and Castillo-Chávez, C. A general solution of the problem of mixing subpopulations, and its application to risk-and age-structured epidemic models for the spread of AIDS, *IMA J. of Mathematics Applied in Med. and Biol.*, **8**, 1-29 (1991).

[9] Castillo-Chávez, C., Song, B. and Zhang, J. An epidemic model with virtual mass transportation: the case of smallpox in a large city, *Bioterrorism: Mathematical Modeling Applications in Homeland Security, SIAM Frontiers in Applied Mathematics*, edited by H.T. Banks and C. Castillo-Chávez (SIAM, Philadelphia, 2003), **28**, 173-197.

[10] Castillo-Chávez, C., Velasco-Hernández, J. X. and Fridman, S. Modeling contact structures in biology, in *Frotiers of Theoretical Biology, Lecture Notes in Biomathematics*, edited by S. A. Levin (Springer-Verlag, Berlin-Heidelberg-New York, 1994), **100**, 454-491.

[11] Chowell, G. and Castillo-Chávez, C. Worst-case scenarios and epidemics,in *Bioterrorism: Mathematical Modeling Applications in Homeland Security, SIAM Frontiers in Applied Mathematics*, edited by H.T. Banks and C. Castillo-Chávez (SIAM, Philadelphia, 2003), Vol. 28, p.35.

[12] Chowell, G., Hyman, J.M., Eubank, S., Castillo-Chavez, C. Scaling laws for the movement of people between locations in a large city. Physical Review E **68**, 066102 (2003).

[13] Del Valle, S., Hethcote, H., Hyman, J.M., and Castillo-Chávez, C. *Effects of Behavioral Changes in a Smallpox Attack Model,* Mathematical Biosciences. **195**, pp. 228-251, 2005.

[14] Dezso, Z., and Barabási, A.-L. *Halting viruses in scale-free networks*, Rev. Lett. **65**, 055103 (2002).

[15] Dietz, K. and Heesterbeek, J.P.A. Bernoulli was ahead of modern epidemiology. *Nature*, **408**, 513-514 (2000).

[16] Eguíluz, V.M., and Klemrn, K. *Epidemic threshold in structured scale-free networks*, Phys. Rev. Lett. **89**, 108701 (2002).

[17] Faloutsos, M., Faloutsos, P., Faloutsos, C. *On Power-Law Relationships of the Internet topology*, SGCOMM (1999).

[18] Fenner, F., Henderson, D.A., Arita, I., Jezek, Z., Ladnyi, I.D. Smallpox and Its Eradication (World Health Organization, Geneva),1988.

[19] Halloran, M.E., Longini Jr., I.M., Nizam, A., and Yang, Y. Containing Bioterrorist Smallpox, *Science Magazine*, **298**, 1428-1430 (2002).

[20] Henderson, D.A. About the first national symposium on medical and public health response to bioterrorism, Emerg. Infect. Dis., **5**, 491 (1999).

[21] Henderson, D.A. Smallpox: Clinical and Epidemiologic Features, Emerg. Infect. Dis., **5(4)**, 537-539 (1999).
[22] Henderson, D.A. The looming threat of bioterrorism. *Science*, **283**, 1279-1282 (1999).
[23] Hethcote, H. The mathematics of infectious diseases, *SIAM Rev.*, **42**, 599-653 (2000).
[24] Jacquez, J.A., Simon, C.P., Koopman, J., Sattenpiel, L., Perry, T. Modeling and analyzing HIV transmission: effect of contact patterns, *Math. Biosci*, **92**, 119-199 (1988).
[25] Jeong, H., Tombor, B., Albert, R., Oltvai, Z.N. and Barabási, A.-L. *The large-scale organization of metabolic networks*, Nature **407**, 651-654 (2000).
[26] Kahn, L.H. Smallpox Transmission Risks: How Bad?, *Science*, **297**, 50 (2002).
[27] Kaplan, E.H., Craft, D.L., and Wein, L.M. *Emergency response to a smallpox attack: The case for mass vaccination, Proceedings of the National Academy of Science U.S.A.*. **99**,17, pp. 10935-10940, 2002.
[28] Klemrn, K. and Eguíluz, V.M. *Highly clustered scale-free networks*, Phys. Rev. E **65**, 036123 (2002).
[29] Kumar, R., Raghavan, P., Rajagopalan, S., Sivakumar, D., Tomkins, A.S., Eli UpfalProc (200). 19th ACM SIGACT-SIGMOD-AIGART Symp. Principles of Database Systems, PODS.
[30] Lai Y.-C. (private communication).
[31] Larsen, R. Smallpox: Right Topic, Wrong Debate, *J. Homeland Security*, July 14,2002, http://www.homelandsecurity.org/ HLSCommentary/20020725.htm. Accessed January 31, 2003.
[32] Liljeros, F., Edling, C.R., Amaral, L.A.N., Stanley, H.E. and Aberg, Y. *The web of human sexual contacts*, Nature (London) **411**, 907 (2001).
[33] Liu, Z., Lai, Y.-C., Ye, N., and Dasgupta, P. Connectivity distribution and attack tolerance of general networks with both preferential and random attachments *Phys. Let. A*, **303**, 337-344 (2002).
[34] May, R.M., and Lloyd, A.L. Infection dynamics on scale-free networks, *Phys. Rev. E*, **64**, 066112 (2001).
[35] Meltzer, M.I., Damon, I., LeDuc, J.W., and Millar, D. Modeling potential responses to smallpox as a bioterrorist weapon, *Emerg. Infect. Dis.*, **7**, 959-969 (2001) .
[36] Milgram, S. *The small world problem*, Psychol. Today **2**, 60-67 (1967).
[37] Moore, C. and Newman, M.E.J. *Epidemics and percolation in small-world networks*, Phys. Rev. Lett. 61, 5678-5682 (2000).
[38] Newman, M.E.J. *The Structure of Scientific Collaboration Networks*, Proc. Natl. Acad. Sci. **98**, 404-409 (2001).
[39] Newman, M.E.J. *Who is the best connected scientist? A study of scientific coauthorship networks*, Phys Rev. E64 (2001) 016131; Phys.Rev. E **64**, 016132 (2001).
[40] Newman, M.E.J. The structure and function of complex networks, *SIAM Rev.*, **45**, 2, 167-256 (2003).
[41] Newman, M.E.J. Mixing patterns in networks, *Phys. Rev. E*, **67** , 026126 (2003).
[42] Newman, M.E.J. and Watts, D.J. *Renormalization group analysis of the small-world network model*, Phys. Lett. A **263**, 341-346 (1999).
[43] Nold, A. Heterogeneity in disease-transmission modeling, *Math. Biosci*, **52**, 227-240 (1980).
[44] Pang, X., Zhu, Z., Xu, F., Guo, J., Gong, X., Liu, D., Liu, Z. Chin, D.P., and Feikin, D.R. Evaluation of control measures implemented in the severe acute respiratory syndrome outbreak in Beijing, *J. Am. Math. Assoc.*, **290**, 3215-3221 (2003).
[45] Pastor-Satorras, R. and Vespignani, A. *Epidemic spreading in scale-free networks*, Phys. Rev. Lett. **86**, 3200 (2001).
[46] Pastor-Satorras, R. and Vespignani, A. *Immunization of complex networks*, Phys. Rev. Lett. **65**, 036104 (2002).
[47] Rotz, L.D., Khan, A.S., Lillibridge, S.R., Ostroff, S.M., Hughes, J.M. Public Health Assessment of Potential Biological Terrorism Agents, *Emerg. Infect. Dis.*, **8**, 2, 225-229 (2002).
[48] Stauffer, D. and Aharony, A. Introduction to Percolation Theory, Revised 2nd Edition, (2002).
[49] Watts, D.J. and Strogatz, S.H. *Collective Dynamics of 'small-world' networks*, Nature **383**, 440-442 (1998).
[50] Wehrle, P.F., Posch, J., Richter, K.H., Henderson, D.A. An airborne outbreak of smallpox in a German hospital and its significance with respect to other recent outbreaks in Europe, *Bull World Health Organ.*, **43**, 669-679 (1970).

[51] Centers for Disease Control web site. What CDC is Doing to Protect the Public From Smallpox. < http://www.bt.cdc.gov/agent/smallpox/prep/cdc-prep.asp>

Mathematical Modeling and Analysis (MS B284), Los Alamos National Laboratory, Los Alamos, NM 87545, USA
E-mail address: chowell@lanl.gov

Center for Applied Mathematics, Cornell University, 657 Rhodes Hall, Ithaca NY 14853, USA
E-mail address: ariel@cam.cornell.edu

Simulation Science CCS-5 (MS M997) Los Alamos National Laboratory, Los Alamos NM 87545, USA
E-mail address: sdelvall@lanl.gov

Biological Statistics and Computational Biology, Cornell University, 432 Warren Hall, Ithaca NY 14853, USA
E-mail address: fas9@cornell.edu

Department of Mathematical Sciences, Montclair State University, Upper Montclair, NJ 07043, USA
E-mail address: songb@mail.montclair.edu

Mathematical Modeling and Analysis (MS B284), Los Alamos National Laboratory, Los Alamos, NM 87545, USA
E-mail address: hyman@lanl.gov

Department of Mathematics, University of Iowa, 14 MacLean Hall, Iowa City, IA 52242
E-mail address: herbert-hethcote@uiowa.edu

Department of Mathematics and Statistics, Arizona State University, PO BOX 871804, Tempe, AZ 85287, USA
E-mail address: chavez@math.asu.edu